Numerical Simulation of Tidal Currents in an Island Basin with Variational Boundaries

By

Xiaoling ZHAO, Iehisa NEZU† and Hiroji NAKAGAWA††

(Received March 17, 1992)

Abstract

In this paper, we describe a numerical model that is called "the crevice method" using a triangular mesh difference to simulate tidal currents in an island basin with a large area of beach; the land boundaries move with the shift of the tide, and with geometrically complex boundaries. This model is based on shallow water momentum and continuity equations. For simulating variational boundaries, crevices which are artificially imagined are erected all over the shallows where the bed elevations are not lower than the lowest tidal level and where the water depth in the crevices changes with the ascent and descent of the tidal levels. For simulating a flow field within geometrically complex island boundaries, especially in flow circumstances near the islands, the triangular mesh difference is adopted in this model. The second derivative of u, v and ζ with respect to time and the semi-implicit scheme are used in the triangular mesh difference for the purpose of increasing stability and accuracy, Practical calculation of tidal currents shows that this model has the advantages of better stability, higher accuracy, shorter calculation time, and it saves computer memory. The calculated results coincide reasonably with the measured ones.

1. Introduction

The finite difference method (FDM) and the finite element method (FEM) are often used in simulating tidal currents. The former usually adopts regular rectanglar mesh, therefore, it does not easily fit complex geometries (e.g. Jean et al., 1982 and Wensen et al., 1988). The latter uses the triangular mesh, but it nodes more computer memory and longer calculating time because it has to solve large-scale simultaneous equations (e.g. Kawahara et al., 1978 and Wu et al., 1985). In the island basin, there are rather complex boundaries which may lead to large spatial variations of the flow quantity, making accurate numerical representations of them difficult and sometimes impossible. Thacher (1977) has

Research Fellow, Global Environment Engineering, Kyoto University, Kyoto 606, Japan (formerly, Research Assoc. Dalian University of Technology, China)

† Assoc. Professor, Global Environment Engineering, Kyoto University, Kyoto 606, Japan

††Dean, Professor, Global Environment Engineering, Kyoto University, Kyoto 606, Japan

put forward the irregular grid finite difference technique. It shows that irregular difference has the advantages of FDM and FEM. Liuzhi (1987) has employed the finite difference method with unequal lengths of steps and derived a uniform derivative form of the triangular mesh and rectangular mesh. Meakin et al. (1988) has used a curvilinear coordinate in the FDM for simulating the environmental flow with complex geometries. Rodi et al. (1989) have used curvilinear boundary-fitted coordinates and quadrilateral control cells in modeling incompressible flows with geometrically complex boundaries. Variational boundaries are very popular in practical engineering. Small areas of shallows can be excavated to a level lower than the lowest water level and a rough ratio is added or the coastline is moved forward by the equilibrium of the flow quantity. However, this assumption becomes invalid in regions of large areas of shallow beach. Some moving boundary models have been developed (e.g. Gopalakrishnan et al., 1983 and Kawahara et al., 1986). Gopalakrishnan (1989) has employed a continuously deforming grid to have the boundary nodes always on the moving edge of the water body in calculating the flow in regions with large tidal flats. Shi (1986) has employed a comprehensive identification method to determine the new coastline in every step, but it needs more artificial interference and complex calculation. Tao (1984) has employed crevices to model one-dimensional waves creeping against a sloping bank. Wang et al. (1986) also used the crevice model in rectangular mesh and sucessfully modeled a variational boundary. However, he separated the tidal current into two one-dimensional flows in X and Y directions and it did not easily fit complex geometries.

In this study, we apply the crevice method to the triangular mesh difference for modeling tidal currents that have not only a geometrically complex boundary but also a large area of shallows in which the coastline changes as the tide advances and recedes. This model has clear physical concepts, saves computer memory resources and is easy to realize in programs. Crevices can be put up all over the shallows. Therefore, it is very convenient in solving moving boundary problems. The combination of the crevice with the triangular mesh difference has been verified as successful by applying it to the practical simulation of tidal currents.

2. Establishment of Mathematical Models

The governing equations of tidal currents are shallow water equations. Their form will change after the crevices are erected. In this study, the crevices are erected using a different concept from others who employed rectangular mesh and

the crevices were set up in the mesh in an exposed region. First, it is assumed that there are many vertical and horizonal crevices in all of the shallows and that they extend to the water area. The bottom elevations of the crevices are lower than the lowest tidal level. Therefore, seawater in the water area can flow into the shallows. We are not concerned with the actual flow in the realistic crevices. The purpose of the crevices is only to draw water through the shallows to the fixed boundary under the condition of the equilibrium of water quantity. Afterwards, water in the crevices is spread all over the shallows to create a continuous water region. Then we use the triangular mesh splitting on the whole basin. The difference from the preceding methods in putting up the crevices is the density of the crevices and their position. Fig. 1 shows the positional relations of the mesh and the crevices. For obtaining the crevice parameters at each point on the triangular mesh, the density of the crevices should far exceed that of the triangular mesh. Assume the length of the shortest side of the mesh is L and the length of distance between the crevices is Lc. Let $Kc=Lc/\mathrm{L}$ (in Fig. 1, $Kc=1/50$); we can draw the conclusion that the error from the positional difference of the intersecting points of the mesh and that of the intersecting points of the crevices in calculating the water depth can be ignored, provided the coefficient Kc is small enough.

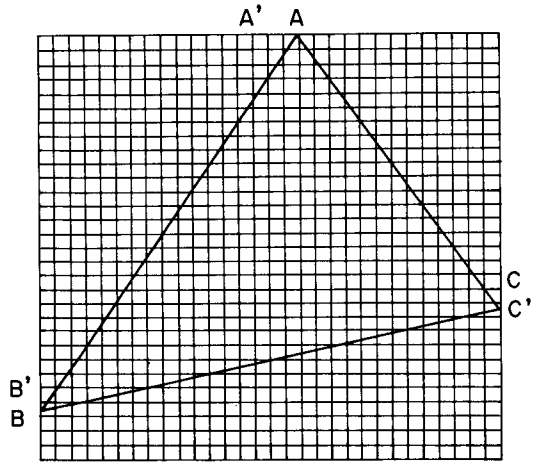

Fig. 1 Arrangement of the crevices

DEFINITION OF CREVICES

In Fig. 1, the crevices that are artificially imagined are set up in x and y

directions in the whole shallows. The shape of the crevices is shown in Fig. 2. The crevice width per unit width is defined as

$$f(z)=\begin{cases}\varepsilon+(1-\varepsilon)\exp\left[\alpha(z-z_b)\right] & z\leqq z_b\\ 1.0 & z>z_b\end{cases} \tag{1}$$

where, ε and α are the parameters of the crevice, z is the water level, z_b is the elevation of the seabed, z_s is the elevation of the water surface and z_0 is the elevation of the crevice bottom.

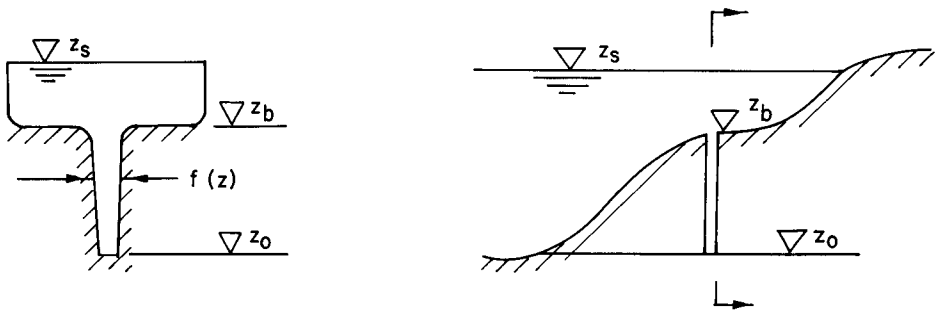

Fig. 2 Definition of the crevice function

ESTABLISHMENT OF GOVERNING EQUATIONS AFTER THE CREVICES ARE CONSIDERED

For deriving the governing equations after the crevices are considered, an arbitrarily chosen element is shown in Fig. 3. The sectional areas vertical to the x and y axes are defined as $A_x(z)$ and $A_y(z)$ respectively.

$$A_x(z)=\int_{z_0}^{z_s} f\ (z)\ dydz=dy\int_{z_0}^{z_s} f\ (z)\ dz$$

$$A_y(z)=\int_{z_0}^{z_s} f\ (z)\ dxdz=dx\int_{z_0}^{z_s} f\ (z)\ dz$$

The water depth on the shallows can be simplified as

$$h_x=\frac{A_x(z)}{dy}\quad,\quad h_y=\frac{A_y(z)}{dx}$$

Therefore, $h_x=h_y$. Let $h=h_x=h_y$, h is the water depth in the shallows and it can be written as

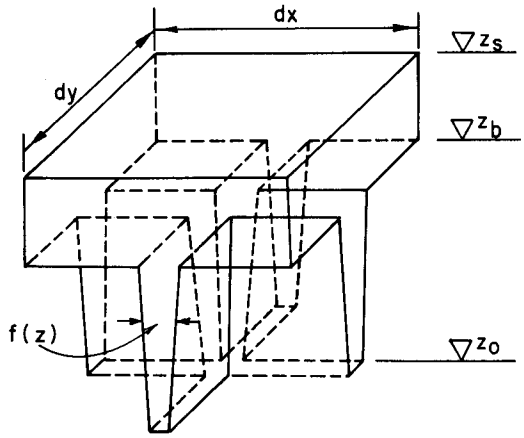

Fig. 3 An element after the crevices being set up

$$h=\begin{cases}\varepsilon(z_s-z_0)+\dfrac{1-\varepsilon}{\alpha}\exp[\alpha(z_0-z_b)]\{\exp[\alpha(z_s-z_0)-1]\} & \text{for } z_s\leqq z_b\\ (z_s-z_b)+\varepsilon(z_b-z_0)+\dfrac{1-\varepsilon}{\alpha}\{1-\exp[\alpha(z_0-z_b)]\} & \text{for } z_s>z_b\end{cases} \tag{2}$$

A new element that is shown in Fig. 4 can be formed by this simplification. Its bottom elevation is a function of the water surface elevation. Here, we use z_b^* to express its bottom level; z_b^* can be expressed as

$$z_b^*=z_s-h \tag{3}$$

It will change in every calculated time step. We use Fig. 5 to simulate this change.

Integrating from the bottom to the surface for the simplified element in Fig. 4 and conducting the average in the vertical direction, the Navier-Stokes equations can be changed into the following form

$$\left.\begin{aligned}&\frac{\partial u}{\partial t}+u\frac{\partial u}{\partial x}+v\frac{\partial u}{\partial y}-fv+g\frac{\partial \zeta}{\partial x}+\frac{guQ}{c^2h}=0\\&\frac{\partial v}{\partial t}+u\frac{\partial v}{\partial x}+v\frac{\partial v}{\partial y}+fu+g\frac{\partial \zeta}{\partial y}+\frac{gvQ}{c^2h}=0\end{aligned}\right\} \tag{4}$$

which are momentum equations which include the influence of the crevices. Where ζ is the water level; u and v are the velocities in x and y directions respectively; $c=\frac{1}{n}h^{1/6}$; $Q=\sqrt{u^2+v^2}$. For elements in Fig. 4, the net discharge entering the element is

$$-\frac{\partial(uA_x)}{\partial x}dx-\frac{\partial(uA_y)}{\partial y}dy$$

and the increase in the discharge is

$$(\frac{\partial\zeta}{\partial t}-\frac{\partial z_b^*}{\partial t})\times[f(z)dxdy+f(z)dydx-f(z)dxf(z)dy]$$

where z_b^* is changed with ξ on the beach. The total change of water volume in z direction can be obtained by using the element shown in Fig. 3, because z_0 is a constant.Let $F(z)=2f(z)-[f(z)]^2$. A continuous equation can be obtained on the basis of the conservation law of mass.

$$\frac{\partial\zeta}{\partial t}+\frac{1}{F(z)}\frac{\partial(uh)}{\partial x}+\frac{1}{F(z)}\frac{\partial(vh)}{\partial y}=0 \tag{5}$$

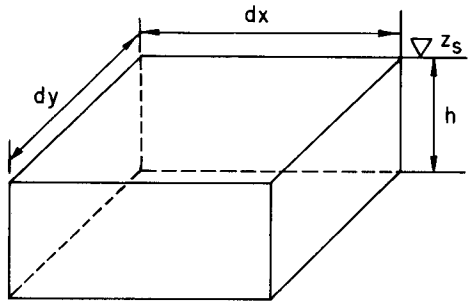

Fig. 4 The simplified element

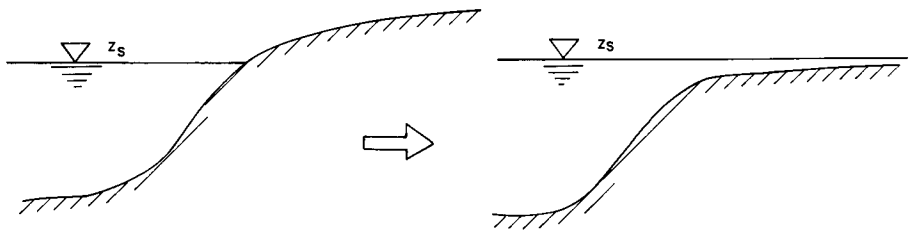

Fig. 5 The water depth on the beach by simplification

3. Numerical Method

SPLITTING FROM OF MATHEMATICAL MODEL

Let the function change linearly in the triangular element

$$f(x,y)=a+bx+cy$$

Hence, $\partial f/\partial x=b$, $\partial f/\partial y=c$. The coefficients b and c can be obtained by substituting the values of points a, b and c of triangle Ⓚ shown in Fig. 6 into the linear equation and solving it; that is

$$\begin{cases} f_a=a+bx_a+cy_a \\ f_b=a+bx_b+cy_a \\ f_c=a+bx_c+cy_c \end{cases}$$

$$b=\frac{1}{|D|}\begin{vmatrix} 1 & f_a & y_a \\ 1 & f_b & y_b \\ 1 & f_c & y_c \end{vmatrix}, \quad c=\frac{1}{|D|}\begin{vmatrix} 1 & x_a & f_a \\ 1 & x_b & f_b \\ 1 & x_c & f_c \end{vmatrix}$$

Here

$$|D|=\begin{vmatrix} 1 & x_a & y_a \\ 1 & x_b & y_b \\ 1 & x_c & y_c \end{vmatrix}=2\Delta_k,\Delta_k \text{ is the area of triangle Ⓚ.}$$

Liu et al. (1987) has determined that the partial derivative in the triangular mesh has the same form as that in the rectangular mesh, that is

$$\left.\frac{\partial f}{\partial x}\right|_{Ⓚ}=\frac{f_e-f_b}{x_e-x_b}, \qquad \left.\frac{\partial f}{\partial y}\right|_{Ⓚ}=\frac{f_a-f_d}{y_a-y_d} \tag{6}$$

Obviously, if the splitting is regular, the triangular mesh difference can turn into the rectangular mesh difference automatically. Therefore, it makes the combination of these two kinds of meshes possible. Their combination is of important significance for simulating the tidal current with a small part of the complex boundary and a large part of the water region.

The derivative at an arbitrary point on the mesh is the average of derivatives of the elements around it.

$$\frac{\partial f}{\partial x}[x_1,y_1]=\sum_{k=1}^{n}[\frac{\partial f}{\partial x}]_k\frac{\Delta_k}{\Delta}, \quad \frac{\partial f}{\partial y}[x_1,y_1]=\sum_{k=1}^{n}[\frac{\partial f}{\partial y}]_k\frac{\Delta_k}{\Delta} \tag{7}$$

where, $\Delta=\sum_{k=1}^{n}\Delta_k$, Δ_k is the area of triangular element Ⓚ. This situation is shown in Fig. 7.

DIFFERENTIAL SCHEME

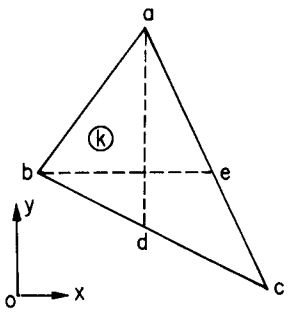

Fig. 6 The derivative in a triangular element

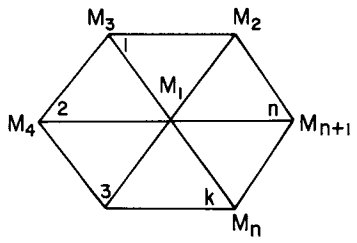

Fig. 7 The derivative in an arbitrary point

This paper adopts the triangular mesh difference in which the second derivative of u, v and ζ with respect to time and the semi-implicit difference scheme are used for increasing the stability of calculation. Let

$$V_i(x,y)=A_i(x,y)+B_i(x,y)t+C_i(x,y)t^2 \tag{8}$$

here $V_1=u$, $V_2=v$, $V_3=\zeta$. A_i, B_i, C_i can be obtained by following conditions

$$t=0:\ U_i=U_i^n,\quad \frac{\partial U_i}{\partial t}=\left(\frac{\partial U_i}{\partial t}\right)^n$$
$$t=\Delta t:\ U_i=U_i^{n+1}$$

By substituting A_i, B_i and C_i, Eq. (8) can be changed into the following form

$$U_i=U_i^n+\left(\frac{\partial U_i}{\partial t}\right)^n+\frac{1}{\Delta t^2}[U_i^{n+1}-U_i^n-\left(\frac{\partial U_i}{\partial t}\right)^n\Delta t]t^2 \tag{9}$$

Eq. (4) can be written as semi-implicit forms as follows:

$$\left.\begin{aligned}&(\frac{\partial u}{\partial t})^{n+1}+u^{n+1}(\frac{\partial u}{\partial x})^n+v^{n+1}(\frac{\partial u}{\partial y})^n-fv^{n+1}\\&\qquad+g(\frac{\partial \zeta}{\partial x})^{n+1}+\frac{gu^{n+1}Q^n}{c^{2hn+1}}=0\\&(\frac{\partial v}{\partial t})^{n+1}+u^{n+1}(\frac{\partial v}{\partial x})^n+v^{n+1}(\frac{\partial v}{\partial y})^n+fu^{n+1}\\&\qquad+g(\frac{\partial \zeta}{\partial y})^{n+1}+\frac{gv^{n+1}Q^n}{c^2h^{n+1}}=0\end{aligned}\right\} \tag{10}$$

Eq. (9) is substituted into Eq. (5), and Eq. (10) and Eq. (5) are integrated from 0 to Δt. The difference equation can be expressed by

$$\left.\begin{aligned}
\zeta_i^{n+1} &= \zeta_i^n - \frac{1}{F(z)}\left\{\frac{\partial}{\partial x}\left[h^n u^n \Delta t + \left(h^n\left(\frac{\partial u}{\partial t}\right)^n + \left(\frac{\partial \zeta}{\partial t}\right)^n u^n\right)\frac{\Delta t^2}{2}\right]\right. \\
&\left. + \frac{\partial}{\partial y}\left[h^n v^n \Delta t + \left(h^n\left(\frac{\partial v}{\partial t}\right)^n + \left(\frac{\partial \zeta}{\partial t}\right)^n v^n\right)\frac{\Delta t^2}{2}\right]\right\} \\
u^{n+1} &= (C_1 \times B_2 - C_2 \times B_1)/DE \\
v^{n+1} &= (C_2 \times A_1 - C_1 \times A_2)/DE
\end{aligned}\right\} \qquad (11)$$

where

$$\begin{aligned}
DE &= A_1 \times B_2 - A_2 \times B_1, \\
A_1 &= 2 + (\partial u/\partial x)^n \Delta t + gQ^n \Delta t/(c^2 h^{n+1}), \\
B_1 &= [(\partial u/\partial y)^n - f]\Delta t, \\
C_1 &= 2u^n + (\partial u/\partial t)^n \Delta t - g\Delta t(\partial \zeta/\partial x)^{n+1}.
\end{aligned}$$

Similarly, the coefficients $A_2 - C_2$ can be obtained.

ANALYSIS OF ERRORS

If a difference equation is converged into a differential equation, the differential equation must satisfy conditions of permissibility and stability. The error of triangular mesh difference is the algebraic sum of the errors produced by splitting of every differential operator.

From previous analysis, we know that the partial derivative at an arbitrary point in the triangular mesh is the average of the partial derivatives of the elements around it. In fact, the partial derivatives of these elements are different from that at this point in these elements. Now, we analyse the errors produced by using the partial derivative of an element to represent that of a point in a triangle.

Eq. (6) can be written as

$$\left(\frac{\partial f}{\partial x}\right)_k = \frac{1}{|D|}\begin{vmatrix} 1 & f_a^k & y_a \\ 1 & f_b^k & y_b \\ 1 & f_c^k & y_c \end{vmatrix} = \frac{1}{2\Delta_k}\left[(y_b - y_c)f_a + (y_c - y_a)f_b + (y_a - y_b)f_c\right]$$

applying it at o point in element Ⓚ using the Tayler formula

$$\left(\frac{\partial f}{\partial x}\right)_0 = \frac{1}{2\Delta_k}\left\{y_{bc}\sum_{m=1}^{\infty}\left(x_{a0}\frac{\partial}{\partial x} + y_{a0}\frac{\partial}{\partial y}\right)^m \frac{f_0}{m!} + y_{ca}\sum_{m=1}^{\infty}\left(x_{b0}\frac{\partial}{\partial x} + y_{b0}\frac{\partial}{\partial y}\right)^m \frac{f_0}{m!}\right.$$

$$+y_{ab}\sum_{m=1}^{\infty}(x_{c0}\frac{\partial}{\partial x}+y_{c0}\frac{\partial}{\partial y})^m\frac{f_0}{m!}\Big\}$$

Therefore, the coefficient of $\partial f_0/\partial x$ is:

$$\begin{aligned}&\frac{1}{2\Delta_k}(y_{bc}x_{a0}+y_{ca}x_{b0}+y_{ab}x_{c0})\\=&\frac{1}{2\Delta_k}(y_{bc}x_a+y_{ca}x_b+y_{ab}x_c)\\=&1\end{aligned}$$

The coefficient of $\partial f_0/\partial y$ is:

$$\begin{aligned}&\frac{1}{2\Delta_k}(y_{bc}y_{a0}+y_{ca}y_{b0}+y_{ab}y_{c0})\\=&\frac{1}{2\Delta_k}(y_{bc}y_a+y_{ca}y_b+y_{ab}y_c)\\=&0\end{aligned}$$

The coefficients of the second derivative are:

$$\begin{aligned}\frac{\partial^2 f_0}{\partial x^2}&:\ \frac{1}{4\Delta_k}(y_{ca}{x_{ba}}^2+y_{ab}{x_{ca}}^2)\\\frac{\partial^2 f_0}{\partial y^2}&:\ \frac{1}{4\Delta_k}(y_{ca}{y_{ba}}^2+y_{ab}{y_{ca}}^2)\\\frac{\partial^2 f_0}{\partial x\partial y}&:\ \frac{1}{2\Delta_k}(y_{ca}x_{ba}y_{ba}+y_{ab}x_{ca}y_{ca})\end{aligned}$$

They are not all zero. Therefore, the partial derivative in this model has $0(h)$ order precision. Moreover, it can be proved that error is the smallest at the center of gravity of a triangle. If $h\to 0$, *then* $0(h^r)\to 0$ because $r\geqq 1$. So the difference equations converge to differential equations.

4. Boundary Conditions

The analytical domain is surrounded by land boundaries, including the island boundaries, and an artificial boundary that is called an open boundary. Generally, the perfectly reflective condition is imposed at the land boundaries.

On the other hand, the velocities normal to the land boundary are zero, that is, $\vec{V}_n=0$, which is shown in Fig. 8; where $x-y$ is the calculating coordinate

and $\lambda-n$ is the boundary coordinate, they are the tangential and the normal directions of the land boundary respectively.

If the velocities are u_i and v_i in a time step, the velocities at the boundary will be corrected by the boundary condition. The transformation from $X-Y$ coordinate to $\lambda-n$ coordinate is

$$\begin{pmatrix}\lambda\\ n\end{pmatrix}=\begin{pmatrix}\sin\theta_i & -\cos\theta_i\\ \cos\theta_i & -\sin\theta_i\end{pmatrix}\begin{pmatrix}x\\ y\end{pmatrix}$$

Here, $u_n=0$, $u_\lambda=u_i\sin\theta_i-v_i\cos\theta_i$. In the next calculated time step, u_λ will be resolved into x and y directions. The normal direction n of the land boundary at cornor points is defined as the normal direction of line ab linked by the middle points of two sides of the boundary elements next to the calculated point i, which is shown in Fig. 9.

Usually, the periodic water elevation and velocity are given at the open boundary. The initial condition is to assume water elevation and velocity to be constant. If the amplitude of tidal functions changes at the open boundary, progressive waves will be generated and propagate towards the land boundary. When they meet the land boundary, they will reflect and the reflected waves will propagate towards the open boundary where they will overlap with the incident waves. Kadama et al (1989) have invented a method to treat incident wave conditions in shallow water equations. The simplest method to determine the open boundary conditions is to measure a few water elevations at controlling points and to calculate the water elevations of the mesh points at the open

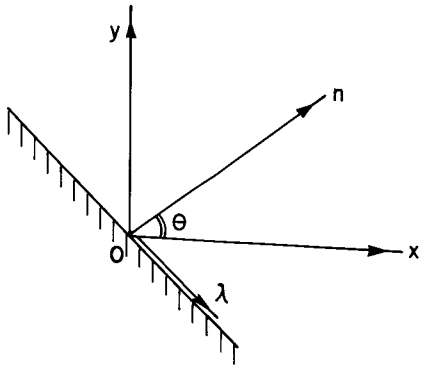

Fig. 8 Land boundary condition

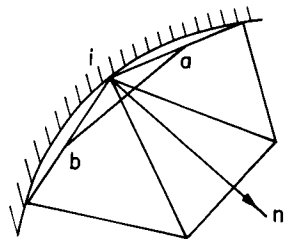

Fig. 9 The direction of n

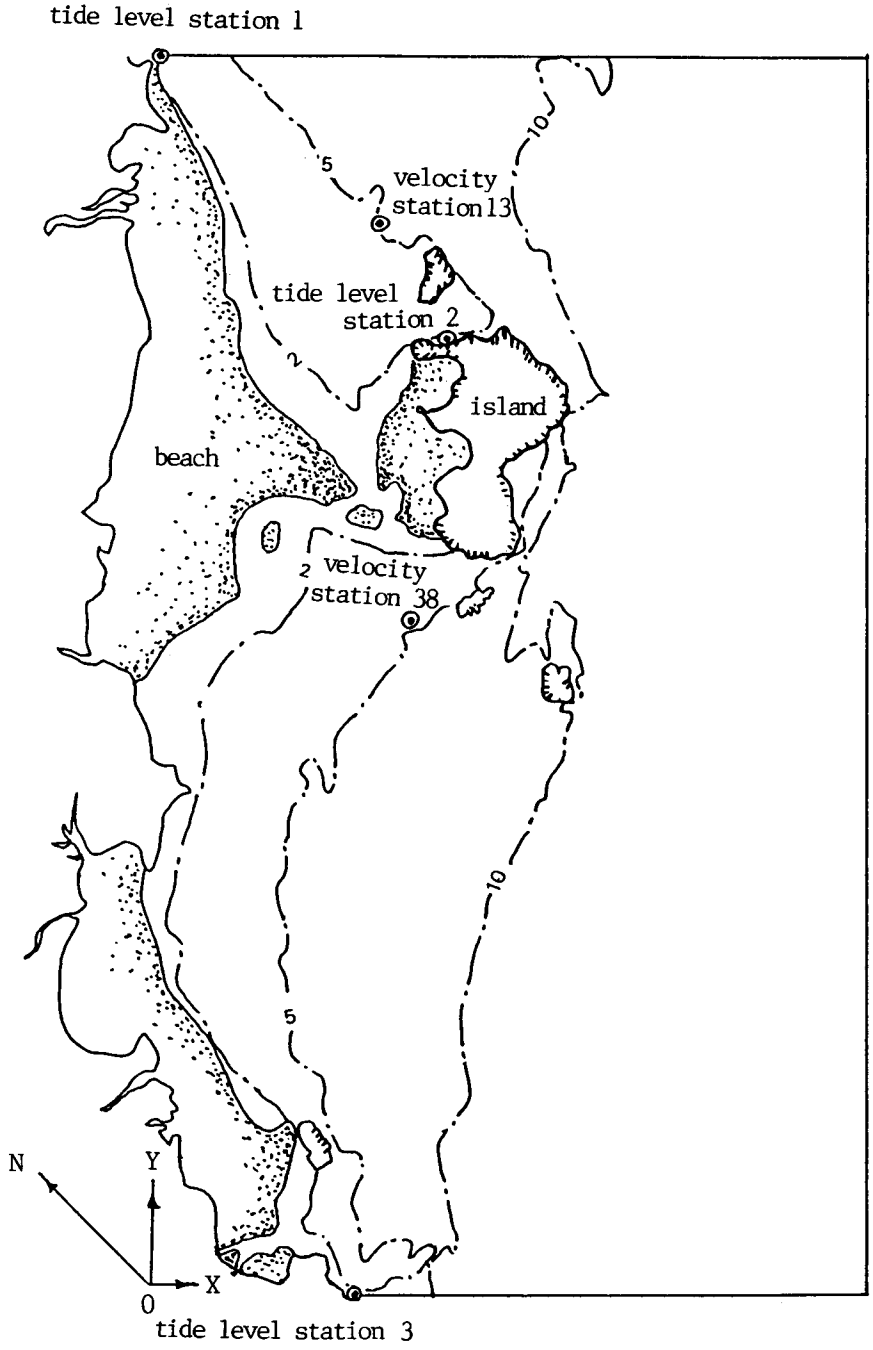

Fig. 10 The map of simulated basin

boundary by the use of linear interpolation. However, before we do this, we must analyse the characteristics of tidal waves in a calculated basin because it can lead to a difference in the tidal phase.

5. Applications of the Numerical Method

STATEMENT OF CALCULATED BASIN

Recently, with the development of islands along the seashore, the complex boundary problems in simulated tidal currents become more and more important. The numerical model of tidal currents in this study has been verified to be a useful way to determine the tidal level and velocity in regions with complex boundaries.

The simulated basin includes three parts of moving boundary regions under tidal forcing, one big island and four small islands. So the boundary conditions have not only moving boundaries but also geometrically complex boundaries. Moreover, there are three open boundaries which are controlled by measured tidal levels. The whole area of the basin is about 565 km^2. The total area of the islands is about 15.79 square km^2. The shallows area is about 90 km^2. The beaches develop from the land boundary on the western side of the basin and the western side of the biggest island to the middle. Tide stations are set up at points 1, 2 and 3. Velocity stations are put up at points 13 and 38. The figure of the calculated basin is shown in Fig. 10.

SIMULATION AND RESULTS

The calculated region is divided into two parts by comparing the bed elevation and the lowest tidal level, one part will be exposed in the calculation and another part will always be in the seawater. We first erect the crevices in all of the shallows in which the bed levels are higher than the lowest water level. Afterwards, the whole basin is split by using the triangular mesh. The triangular mesh has the advantage of arbitrarily densifying, so smaller mesh can be used in complex geometries. Mesh splitting is shown in Fig. 11. Boundary conditions can be classified into open boundaries, fixed boundaries and moving boundaries. The moving boundaries can be turned into fixed boundaries by setting up crevices in the shallows; the velocities normal to the boundaries are zero. The tangential components of the velocity are resolved into u and v for calculation in the next

step. The initial conditions of calculation are

$$\zeta(x, y, t)=\zeta_0(x, y, t),\ u=u_0(x, y, t),\ v=v_0(x, y, t)$$

where, ζ_0, u_0, v_0 are assumed arbitrarily. After a few cycles of computation, the actual initial values can be provided.

The time step is chosen by use of the Courant condition. In Fig. 11, there is the smallest element on the western side of the biggest island. The shortest distance between two mesh points is about 600 m, the average depth in this region is about 1 m, and therefore

$$\Delta t \leqq \frac{\Delta s}{\sqrt{gh}}=\frac{600}{\sqrt{9.8\times 1}} \fallingdotseq 190\ s$$

A time step of 120s is chosen here. The calculating frame is shown in the following:

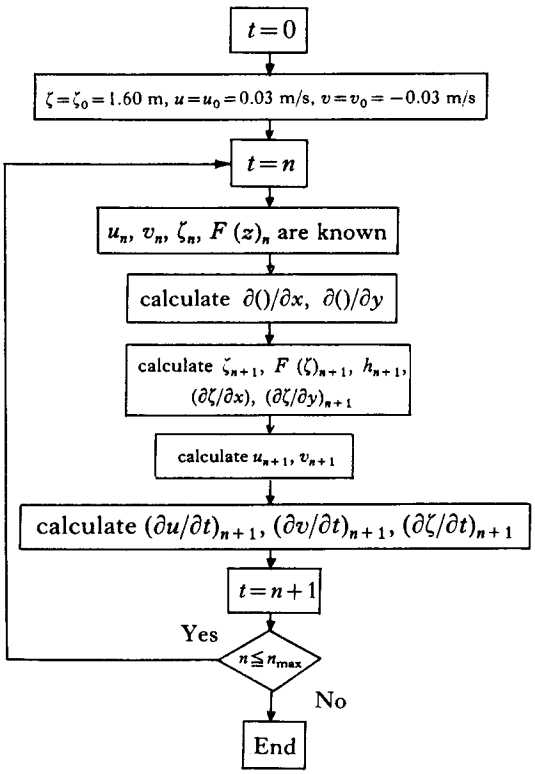

The whole simulated region involves 255 nodes. Among them there are 67 nodes in the crevices (No. 1–67) and 70 nodes on the land boundary (No. 30–99).

Fig. 12 shows a comparison of measured and calculated values of tidal levels.

Fig. 13 shows the comparison of measured and calculated velocity values in

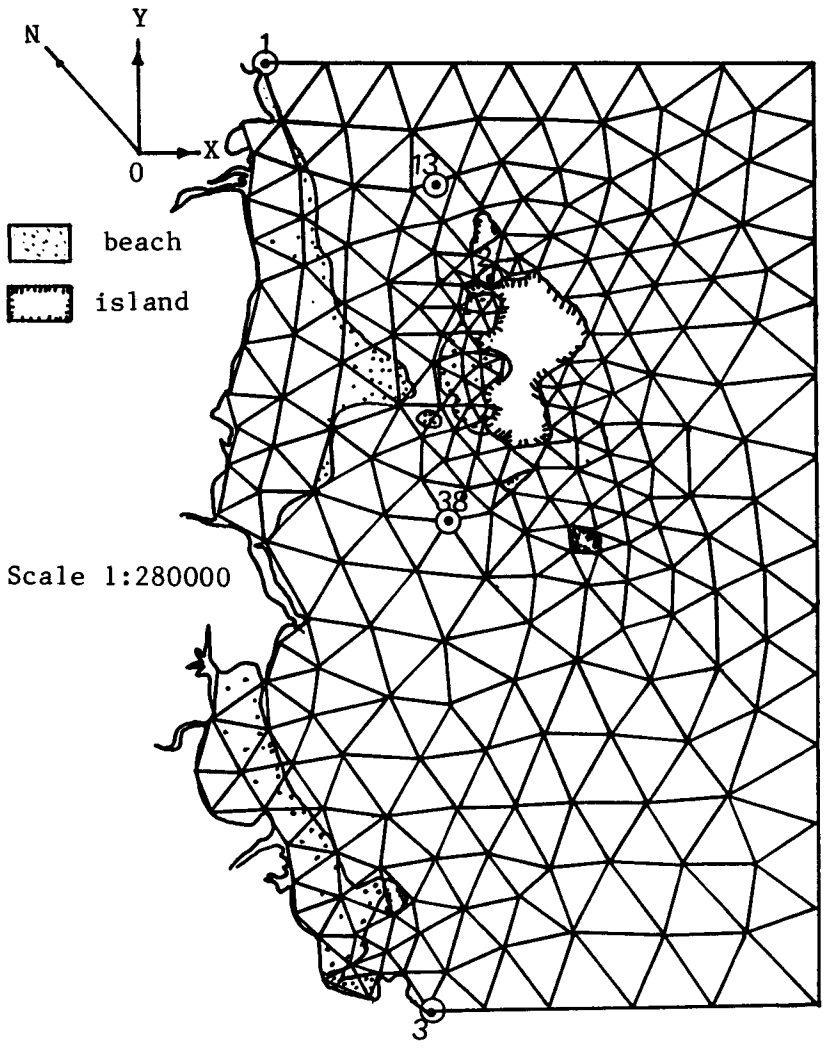

Fig. 11 The figure of scheme splitting

No. 13 and No. 38 stations.

Fig. 14 shows the comparison of calculated values and measured values of velocity directions at No. 13 and No. 38 stations. The calculated values obviously show a left rotation flow, which is consistent with the practical tidal currents. When the tide rises, the main current direction of the tidal current is northwest at point 13 and northeast at point 38. When the tide falls, it is southeast at point 13 and southwest at point 38. From the elliptical figure of the tide, we draw the

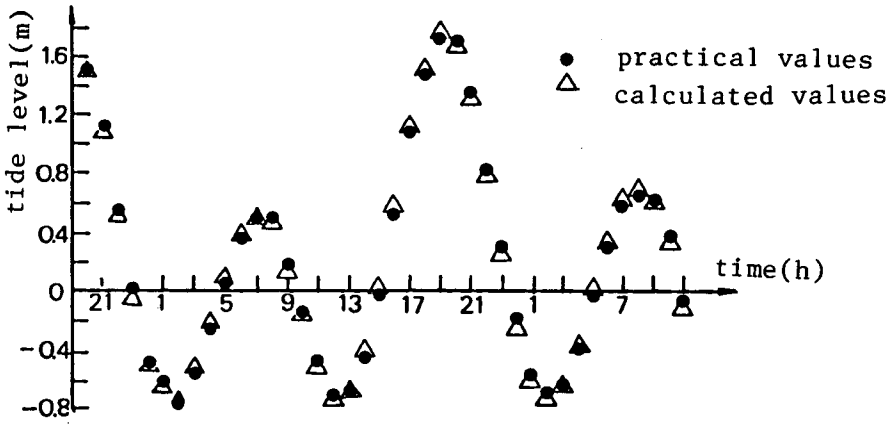

Fig. 12 Comparison of tidal levels at station 2

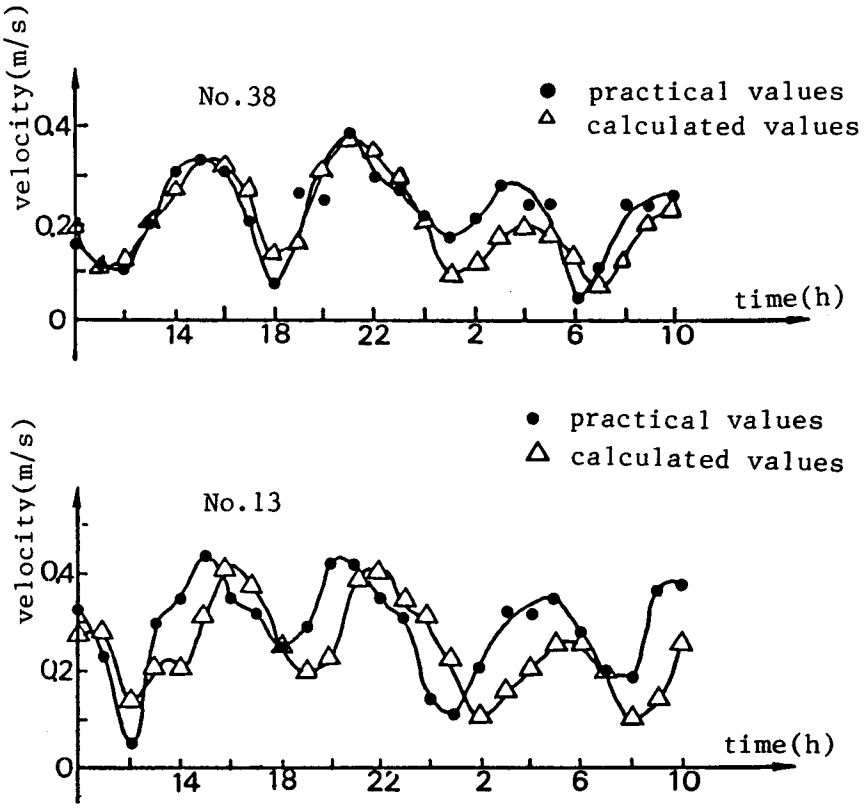

Fig. 13 Comparison of the velocity values at stations 13 and 38

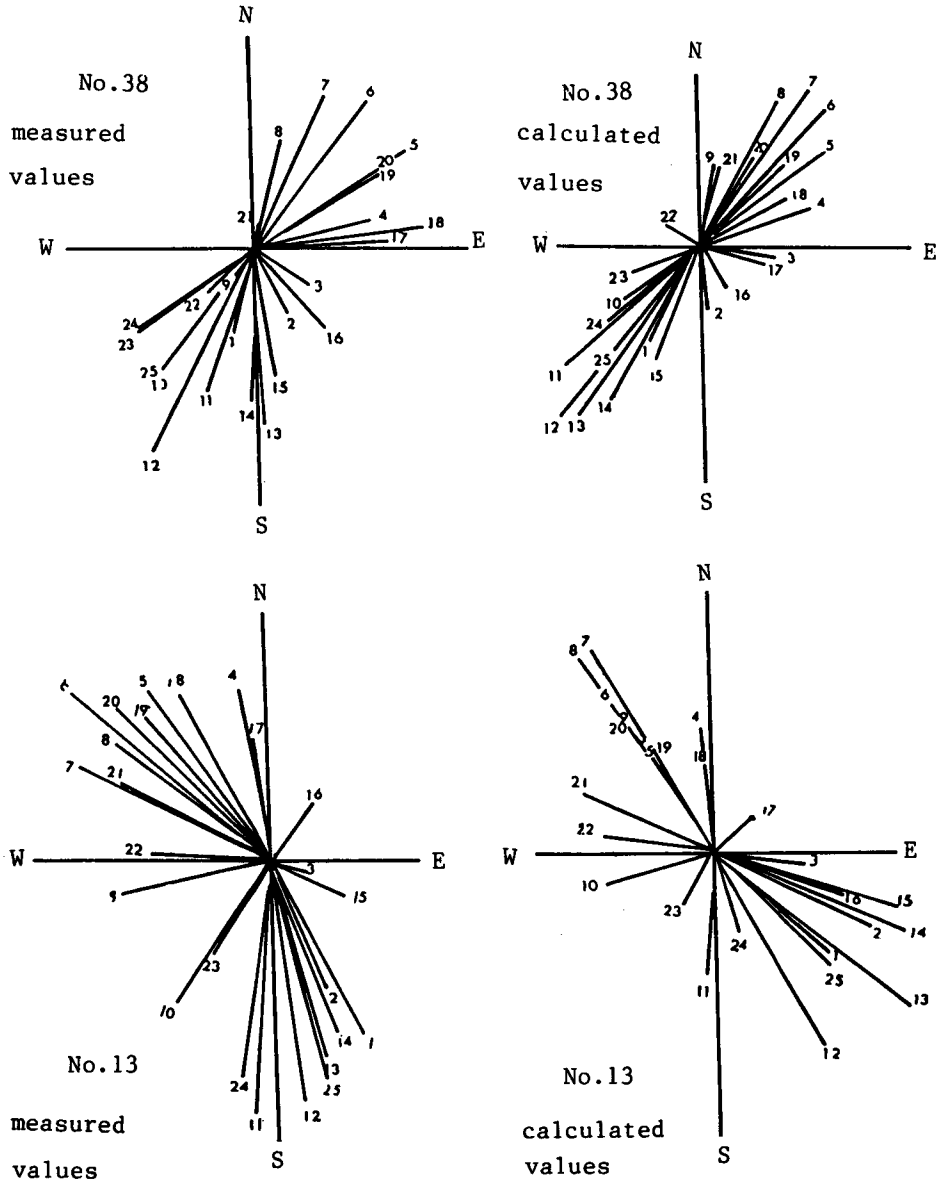

Fig. 14 Comparison of velocity directions at station 13 and 38

conclusion that the directions of computational tidal current coincide well with the measured ones; both their main axes are consistent and the calculated one

has also the characteristic of left rotation.

Fig. 15 shows the flow field in high tide and low tide. From this figure we find that the velocities on the beach are almost zero and the coastline moves towards the water region when the beaches are eexposed. During high tide, the water body flows on the beaches and the coastline moves back.

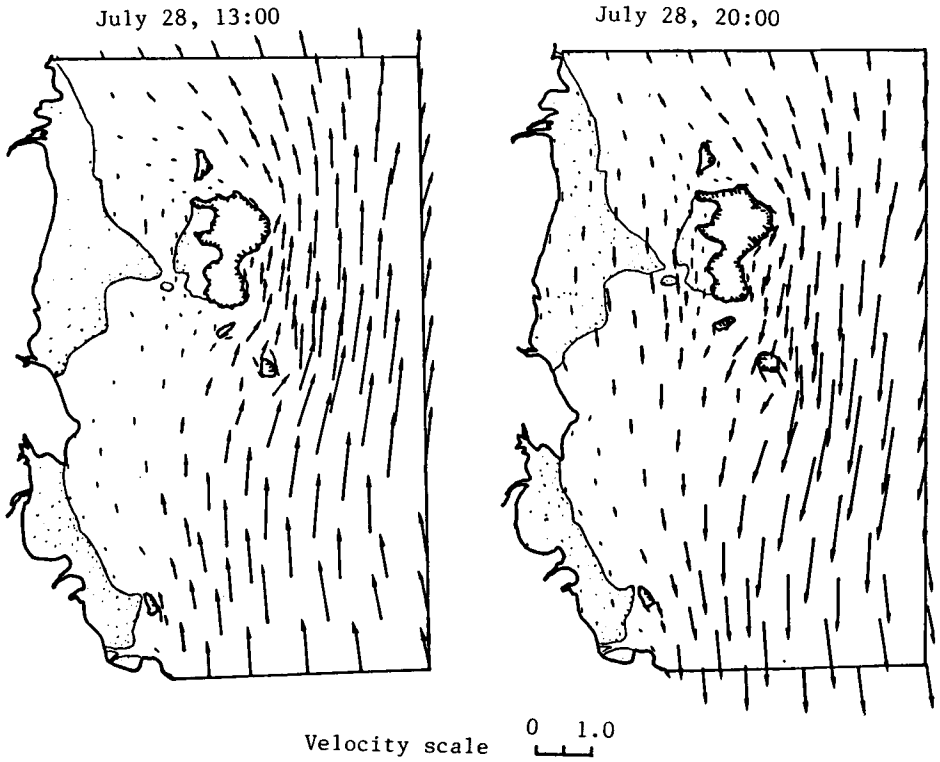

Fig. 15 Flow field figure

6. Discussion

(1). The influence to the balance of water quantity and momentum due to the existence of the crevices

We are concerned with the influence of the crevices on the balance of water quantity and momentum. Because the crevices are erected on the beach, an artificial increase of water body can cause a calculation error. But this error is

very small and its influence on the whole basin flow can be obviated by the following comparison. Moreover, we find that the flow field near the island and the beach is reasonable judging from the flow field figure.

The maximum percentage (K_{in}) of water quantity (Δq_{in}) entering into the crevices, out of the whole water quantity (ΔQ_{in}) entering into the basin per hour when the tide rises, is obtained by

$$K_{in}=\frac{\Delta q_{in}}{\Delta Q_{in}}\times 100\%=1.76\%$$

The maximum percentage (k_{out}) of water quantity (Δq_{out}) going out of the crevices, out of the whole water quantity (ΔQ_{out}) going out of the basin per hour when the tide recedes, is

$$K_{out}=\frac{\Delta q_{out}}{\Delta Q_{out}}\times 100\%=1.80\%$$

(2). Application and dissemination

The flexibility of this model comes from the combination of the crevice model and the triangular mesh difference. No matter how many beaches there are in the basin, the flow in it can be easily simulated. It can not only treat the beach in the calculated basin but also dispose of all of the exposed area under the condition of satisfying the calculating precision. This advantage increases its applied range. For example, there are many islands in the calculated basin, but their areas are very small compared with the area of the whole basin and as we are not extremely concerned with the flow around the islands, we can set up the crevices on the islands to create a water region for calculation.

(3). Choosing the crevice parameters ε and α.

There are two important parameters in the crevice model, that is, ε and α. ε is the value of $f(z)$ when $z\ll z_b$. The value of α determines the slope of the crevice sides. The bigger α is, the quicker the crevice narrows along its depth. Here $0<\varepsilon<1$ and $\alpha<1$. Because the water quantity in the crevices is increased, we hope the error of water quantity will be as small as possible. That means that we want to choose the values of a small ε and a big α. But the calculation will become unstable if the water depth in the shallows is too small. In this paper we assume $\varepsilon=0.02$ and $\alpha=2.3$.

(4). The superiority compared with FEM in simulating complex geometries.

These two kinds of method are flexible in simulating geometrically complex boundaries. But the advantage of this model is evident for large computational regions because it need not solve large scale simultaneous equations and the elements or the nodes have no order. So it can save calculation time and reduce some preparation work.

(5). The advantage compared with the rectangular mesh difference in leading into a closed boundary condition.

Regular rectanglar mesh asks for simplifying a fixed land boundary into a broken line paralleling x and y axes respectively. The boundary condition is that the velocities normal to the land boundary are zero, that is, $u=0$ or $v=0$ at boundary points. But in triangular mesh difference, the velocities normal to the practical boundary are assumed to be zero. So this model not only can model a complex boundary but also can more reasonably introduce a closed boundary condition.

(6). Applying the automatic splitting technique

Automatic splitting is to split the mesh by using a computer after inputting some data about boundary messages in the simulated basin.

The derivative of an arbitrary point is the average of the derivative of elements around it, so we hope the difference of the side lengths in a triangle is not very big. The mesh is densified near complex boundaries. It is the principle of automatic splitting. If it were used in this model, we would reduce large amounts of preparation work and this model would acquire wider application in practical engineering.

Conclusions

The method presented here not only has the advantages of FDM and FEM but also can simulate moving boundaries with complex geometries. The mesh can be densified arbitrarily and the numbers of elements and nodes has no order, which is different from FEM and can reduce some preparation work. It can save more calculation time than FEM or FDM in simulating the tidal current with complex boundaries. The moving boundary model used here is easy to realize in the program.

The crevice method in the triangular mesh, in which the second derivative of u, v and ζ with respect to time and semi-implicit difference scheme are used,

has better stability, especially in the variational boundaries.

By comparing the water quantity per unit time entering into the crevices with that of entering into the basin, the existence of the crevices has less influence on the equilibrium of water quantity and momentum.

The calculated values coincide well with the practical ones.

Appendix I References

Benque, J.P., T.A. Cunge, J. Feuillet, A. Hauguel and F.M. Holly (1982): New Method for Tidal Current Computation, J. Waterway Port Coast. Ocean Eng. Div. ASCE, Vol. 108, pp. 396–417.

Chu, W., B.L. Barker, and A.M. Akbar (1988): Modeling Tidal Transport in the Arabian Gulf, J. Waterway Port Coast. Ocean Eng. Div. ASCE, Vol. 114, pp. 455–471.

Kawahara, M. and K. Hasegawa (1978): Periodic Galerkin Finite Element Method of Tidal Flow, Int. J. Numer. Methods Eng., Vol. 12, pp. 155–127.

Wu, C.S. and P.L.F. Liu (1985): Finite Element Modelling of Nonlinear Coastal Currents, J. Waterway Port Coast. and Ocean Eng., ASCE, Vol. 3, pp. 417–432.

Thacher, W.C. (1977): Irregular Grid Finite Difference Technique: Simulations of Oscillations in Shallow Circulation Basin, J. Phys. Oceangor, Vol. 7, pp. 284–292.

Liu, Z. et al. (1987): The Application of Triangular Mesh Difference in Two-Dimensional Unsteady Flow, Hydraulic Journal, China, Vol. 9, pp. 63–67.

Meakin, R.L. and R.L. Street (1988): Simulation of Environment Flow Problems in Geometrically Complex Domains. Part 1: A General Coordinate Transformation, Computer Methods in Applied Mechanics and Engineering, Vol. 68, pp. 151–175.

Rodi, W., S. Majumdar and B. Schonung (1989): Finite Volume Methods for Two-Dimensional Incompressible Flows with Complex Boundaries, Institute for Hydromechanics, University of Karlsruhe, Karlsruhe, Federal Republic of Germany, Vol. 75, pp. 369–392.

Gopalakrishnan, T.C. and C.C. Tung (1983): Numerical Analysis of a Moving Boundary Problem in Coastal Hydrodynamics, Int. J. Numer. Methods Fluids, Vol. 3, pp. 179–200.

Kawahara, M. and T. Umetsu (1986): Finite Element Method for Moving Boundary Problems in River Flow, Int. J. Number. Methods Fluids, Vol. 6, pp. 365–386.

Gopalakrishnan, T.C. (1989): A Moving Boundary Circulation Model for Regions with Large Tidal Flats, Int. J. Eng., Vol. 28, pp. 245–260.

Shi, L.B. (1986): The Two-Dimensional Hydraulic Calculation in the Estuary with Variational Boundary, People's Zhujiang, China, Vol. 3, pp. 37–44.

Tao, J.H. (1984): The Numerical Simulation of Wave Creeping and Broken in the Beach of Bank, Ocean Journal, China, Vol. 6, pp. 69–75.

Wang, L.X. and S.L. He (1986): The Application of Crevice for Two-Dimentional Flows in Moving Boundary Basin, Hydraulic Journal, China, Vol. 12, pp. 15–21.

Kodama, K. and M. Kawahara (1989): A Method to Treat Incident Wave Conditions in Shallow Water Equations, in S.S.Y. Wang (ed.), Sediment Transport Modelling, ASCE, New Orleans, pp. 178–183.

Appendix II Notation

i = Calculated point
n = Number of calculated time steps
Δt = Calculated time step

t = Calculated time
ζ = Tidal level
u = Velocity of tidal current in x direction
v = Velocity of tidal current in y direction
z = Water elevation in the crevices
h = Water depth
z_b = Elevation of seabed
z_0 = Elevation of crevice bottom
$z_{b'}$ = Elevation of seabed after simplification
z_s = Elevation of water surface
$f(z)$ = Function of the crevice
$F(z)$ = $2f(z)-[f(z)]^2$
α = Parameter of the crevice
θ = Angle of $x-y$ coordinate and $n-\lambda$ coordinate
ε = Parameter of the crevice
Δ_k = Area of a triangular element
k_{in} = Maximum percentage of water quantity entering into the crevices out of the whole water quantity entering into the basin.
Δq_{in} = Water quantity entering into the crevices.
ΔQ_{in} = Water quantity entering into the whole basin.